P H Y S I C A L R E V I E W L E T T E R S

Puckering Stick-Slip Friction Induced by a Sliding Nanoscale Contact

M. V. Rastei,[*] B. Heinrich, and J. L. Gallani

Institut de Physique et Chimie des Matériaux de Strasbourg, CNRS, Université de Strasbourg, F-67034 Strasbourg, France
(Received 28 May 2013; published 19 August 2013)

An atomic force microscope reveals that the sliding of a nanotip on a graphite surface occurs through a nanoscale stick-slip mechanism. The angle between the sliding direction and a stiff crystallographic axis determines the periodicity of the slip events defining domains of various friction properties. The experimental data are interpreted using the reaction rate theory, with the energy barrier driven by a local deformation of the surface and a thermally activated relaxation.

Friction is one of the most fundamental and ubiquitous physical processes. When two bodies in contact slide with respect to each other, friction activates a complex energy transfer at interface. For instance, part of the kinetic energy of the sliding body converts into heat increasing the vibrations of the interface atoms. The heat then dissipates towards the bulk through the contribution of electrons, phonons, and electron-phonon coupling [1–3]. The conversion of kinetic energy is nowadays analyzed by considering a quantized stick-slip motion with atomic periodicity [4]. Since the first observation of this process [5], it became clear that our understanding of the nanoscale friction relied on the identification of friction mechanisms and their realm of validity [6–9].

Recently, atomic-scale friction experiments conduced on graphene samples revealed a marked distortion of the crystalline lattice and a tilt of the friction loops [10]. By finite element modeling, it was predicted that lattice distortions could arise from an out-of-plane deformation of the surface in front of the scanning tip, i.e., a "puckering effect" [10]. This effect was also suggested as contributing to the friction characteristics of a rippled graphene sheet [11]. These studies clearly point out a nanoscale mechanism which enhances friction at the surface of thin lamellar materials. Nevertheless, direct evidence of the puckering effect has not been reported yet. Here, we present the first experimental observation of the puckering-induced nanoscale friction at a graphite surface. We show that puckering generates nanoscale stick-slip processes assigned to a periodic deformation of the contact region followed by a thermally activated relaxation. As these processes depend on the stiffness difference between the crystal axes, they induce a noticeable friction heterogeneity at the graphite surface.

The measurements were performed with a Veeco (now Bruker) atomic force microscope (AFM) operating below 10^{-4} mbar and at room temperature. The (0001) surface of highly oriented pyrolytic graphite was cleaned by repeated exfoliations using an adhesive tape. All data reported here were obtained by recording the friction force microscopy (FFM) signal while scanning along the cantilever axis. Several silicon AFM probes with normal spring constants

of the order of 0.01 N/m were used. To avoid wear of the tip apex, the normal force was kept in the tenth of a nN range.

Figure 1(a) shows a FFM image acquired at the graphite surface. The image reveals stripe patterns grouped in domains of hundreds of nanometers wide. Single or multiple domains can occupy an atomic terrace. In Fig. 1(a) three such domains are labeled Θ_1, Θ_2, and Θ_3. Stripe patterns
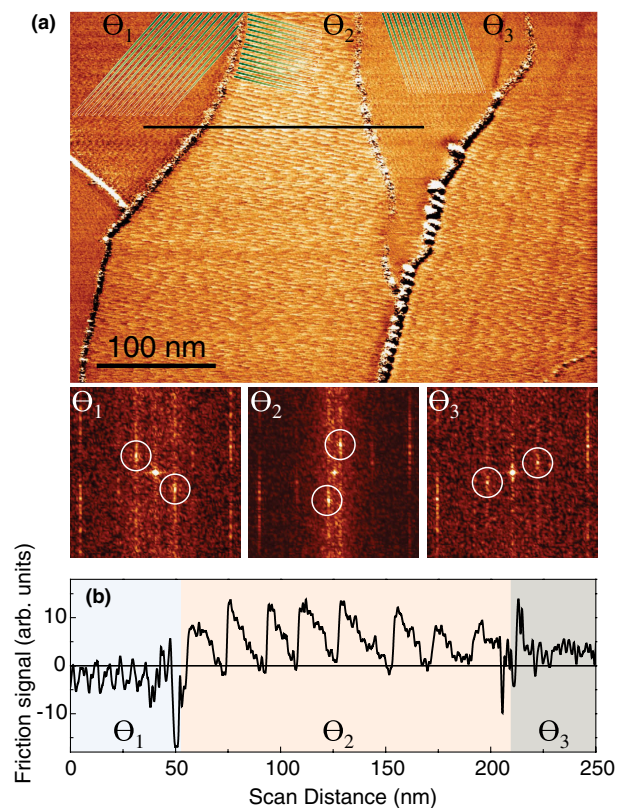

FIG. 1 (color online). (a) FFM backward image (500×350 nm^2) of graphite surface along with FFT images corresponding to the domains labeled Θ_1, Θ_2, and Θ_3. Green lines partly covering the domains indicate the direction of the stripes. The encircled bright spots in the FFT images are generated by the spatial periodicity of the stripes. (b) Scan profile along the line shown in (a).
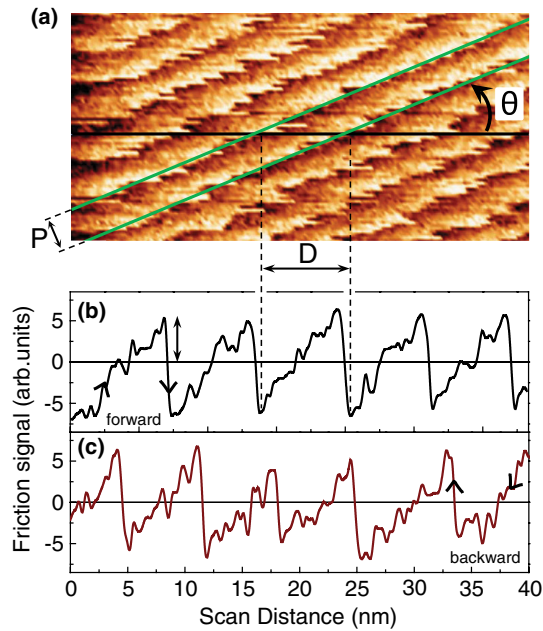
FIG. 2 (color online).   (a) FFM forward image (40×20 nm^2) showing the stripe-pattern structure in an individual domain. θ indicates the direction of the stripes with respect to the horizontal fast-scan direction. P is the periodicity of stripes as can be evaluated by FFT. D shows the scan distance between two consecutive slip events. Zero-centered forward (b) and backward (c) scan profiles, along the horizontal line shown in (a). The vertical double-ended arrow indicates a slip height measured with respect to zero.
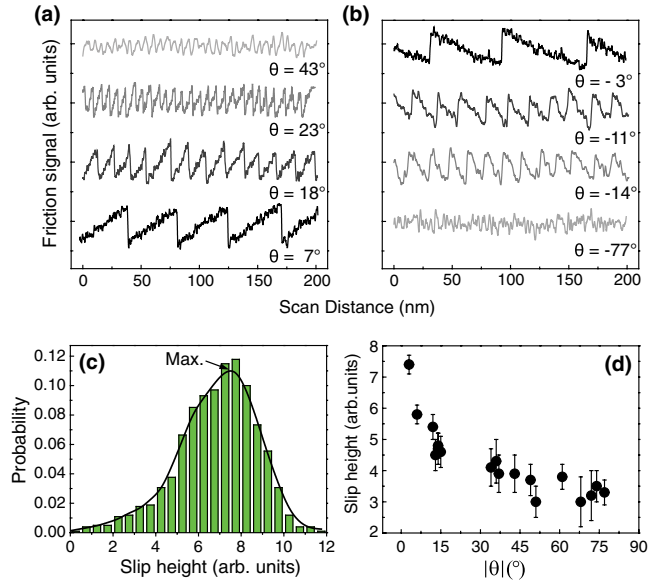

FIG. 3 (color online).   (a) and (b) Forward scan profiles extracted from different domains. (c) Probability for a slip to occur at a certain torsion of the cantilever (slip height) computed from 1010 slip events and for a domain of $|\theta| = 3°$. The black curve is a smooth line through the data. (d) Slip height corresponding to the maximum probability compiled from domains of different θ (scan velocity: 0.1 μm/s, load: 0.4 nN).

are not observed by noncontact AFM or by scanning tunneling microscopy. These periodic stripes must therefore reflect an effect induced by the line-by-line scan of the contacting AFM tip. The direction (θ) and the spatial period (P) of the stripes, as defined in Fig. 2(a), can easily be obtained by performing fast Fourier transform (FFT) analyses (see Sec. 1 in Ref. [12]). FFT images corresponding to the three domains are shown in the lower part of Fig. 1(a). We find $\theta_1 = 47°$, $\theta_2 = -13°$, and $\theta_3 = -69°$. Hence, the angular difference $\Delta\theta_{21} = 60°$ and $\Delta\theta_{32} = 56°$. These differences strongly recall the symmetry of the (0001) surface. The deviation of $\Delta\theta_{32}$ from the ideal value of 60° is due to the presence of a grain boundary between Θ_2 and Θ_3.

To unveil the origin of the stripes, we show in Fig. 1(b) a scan profile across the three domains labeled in Fig. 1(a). The profile reveals a sawtoothlike shape, which at this scale is particularly visible across Θ_2. Such a shape is reminiscent of atomic stick-slip friction, where each tooth comprises a sloped region (stick) followed by an abrupt decrease of the signal (slip) [5]. Although the data are acquired with the cantilever axis along the fast-scan direction, the stick-slip profiles indicate a torsion of the cantilever, suggesting a deviation of the tip from the scan direction. Note that forward and backward scans twist the cantilever in opposite directions [Figs. 2(b) and 2(c)]. The assembly of sawtooth profiles along the slow-scan axis produces the stripes

observed in FFM images. This can easily be deduced when looking, for instance, at the irregular stripe edges in high-resolution low-scale FFM images [Fig. 2(a)].

Figures 3(a) and 3(b) show that the distance (D) between consecutive slips, as well as the sign of the slopes corresponding to the stick parts of the profiles depend on the sign of θ. The profiles extracted from domains with $0 < \theta < 90°$ show positive stick slopes [Fig. 3(a)], while those obtained from domains with $-90° < \theta < 0$ have negative stick slopes [Fig. 3(b)]. Moreover, the analysis of individual domains shows that the slip-height distribution follows an asymmetric bell-shaped curve [Fig. 3(c)]. Such a distribution can be seen as the probability for a slip to occur at a certain torsion of the cantilever [13]. The slip height corresponding to the probability maximum is plotted as a function of θ (different domains) in Fig. 3(d). As observed, it significantly decreases with increasing θ, suggesting an angular dependence of friction with a periodicity of 180° value also encountered for rippled graphene [11].

In contrast with atomic stick-slip friction, where slip events are spaced apart by interatomic distances [5], the distance D between adjacent slips extends here over several nanometers [Fig. 2(a)]. Currently, no friction model includes mechanisms that can explain such extended nanometric stick phases. However, by performing experiments on single and multilayer graphene sheets, Lee *et al.* measured tilted friction loops in the first few nanometers of sliding due to the puckering effect [10]. Additionally, their finite element modeling simulations indicated that the tip

pushed the puckered region forward. In this picture, one could expect the puckering to relax if the elastic force stored in the tip-cantilever probe became comparable with the tip adhesion. This would give rise to nanoscale stick-slip events as reported in the present Letter. Moreover, simulations showed a puckering effect even for the thickest samples examined [10]. These facts speak in favor of a puckering phenomenon which occurs at the same scale as the friction mechanism observed here at the surface of bulk graphite. Alternatively, although in vacuum, various adhesive forces may, in principle, contribute to the tip sticking to the graphite surface. However, the homogeneous twofold stripe pattern observed here over a domain indicated a dominant contribution coming from the crystal structure.

   To explain our experimental observations, we therefore propose a model based on the puckering friction mechanism introduced by Lee *et al.* [10]. Firstly, in order to account for the θ angles observed here, we consider an asymmetric puckering in front of the sliding tip; i.e., the ridge of the puckered region lies along the local stiffest direction (presumably a zigzag or armchair direction). At the beginning, one then expects the tip to spend less energy following the stiff direction than to get over the puckered region. Secondly, the change of the stick-slope sign at $\theta = 0°$ [Figs. 3(a) and 3(b)] can only be explained by assigning the tip deviation along the perpendicular-to-stripes direction. Any other direction would not change the sign for the slopes at $\theta = 0°$. These observations, along with the fact that the slip-height distributions [Fig. 3(c)] indicate thermally activated slips [13], guide us to build the mechanism depicted in Fig. 4(a). Considering that before a slip the tip stands in a metastable state, the distribution function describing the probability to escape is then [13–16]

$$F(f^*) = \frac{3}{2} \frac{f^{*1/2}}{v^*} \exp\left[-f^{*3/2} - (e^{-f^{*3/2}})/v^* \right], \quad (1)$$

where $f^* = (E_b/k_BT)^{2/3}$, with k_BT the thermal energy and E_b the instantaneous barrier height corresponding to the energy needed to overpass the puckered region. The dimensionless velocity v^* accounts in our case, essentially for changes in contact mechanics and barrier height.

   For $E_b \gg k_BT$, a barrier transition is improbable, and the tip linearly displaces along the stiff direction [black-solid line in Fig. 4(a)]. During this phase, E_b gradually decreases because of the potential elastic energy of the twisted cantilever. Note that the scan profiles show a continuous linear ramping of the potential barrier. So, thermally activated transitions are most likely to occur when the scan velocity is low and after the scanner has sufficiently advanced on the scan direction. The 3/2 power law in Eq. (1) indeed accounts for unlikely transitions at weak cantilever torsions [Fig. 3(c)] [13]. Once E_b is sufficiently reduced by the raising torsional energy in cantilever, barrier transition becomes probable due to
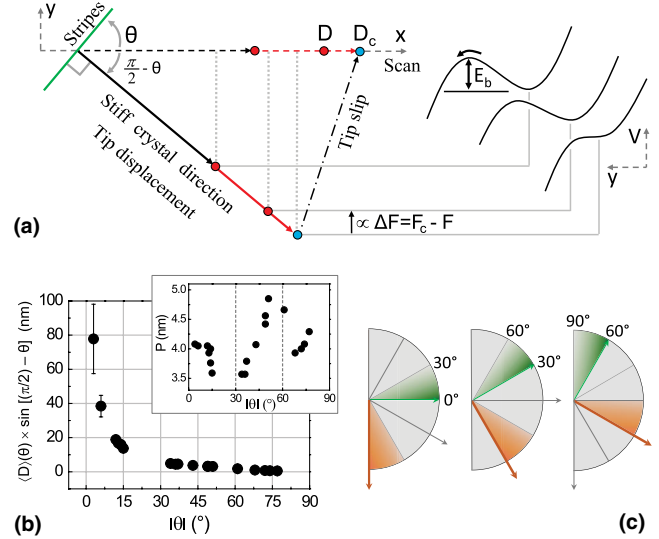

FIG. 4 (color online).   (a) Schematic illustrating the model used to explain a stick-slip process. Red line indicates tip positions where slips are expected. For the sake of clarity, a slip is depicted at the end of the red line only, i.e., at $T = 0$ K. Right: gradual reduction of potential barrier during the stick phase. (b) Mean lateral tip position with respect to the scan axis obtained by analyzing the periodicity of the stripes in domains imaged with the same tip and under the same scanning conditions. Inset: periodicity of stripes vs θ. When not visible, error bars are smaller than the size of the data points. (c) Sketch showing three lattice-induced friction regimes. Green areas: angular intervals spanned by $|\theta|$ angles, as suggested by data shown in (b). Orange areas: corresponding intervals spanned by the stiff direction (orange arrow). Gray arrows indicate the second axis of the same symmetry present in the quadrant.

thermal-induced contact fluctuations. It is important to note here that a transition will be accompanied by a relaxation of the puckered region and to a dissipation of the elastic energy stored into it. The red line in Fig. 4(a) illustrates the interval where transitions are likely. Slips are thus expected throughout this zone, however, with different probability [Fig. 3(c)].

   The time needed before a thermally activated transition takes place is then given by the Kramer's rate $\tau^{-1} = A \exp(-E_b/k_BT)$ [17], where the prefactor describes the damping regime of tip-sample interaction [17,18]. As the tip is in close contact with the surface, A corresponds to the hopping attempt frequency (kHz range) given by the cantilever-tip-nanocontact mechanics [19]. This, again, suggests a high dissipation rate of the tip's kinetic energy into the graphite surface. At $T = 0$ K, a slip event would occur when the barrier has vanished. Hence, as for atomic stick-slip, the mean friction force at zero temperature F_c links E_b to friction force F needed to induce a slip at a finite temperature [20]. More generally, $E_b = K(F_c - F)^{3/2}$ [13], where K depends on the effective stiffness of the cantilever-tip-contact ensemble (c_{eff}), the width (a), and

initial barrier height right after the puckering formed. Provided that c_{eff} and a can be determined, an estimation of the initial barrier height becomes possible, as has been done for atomic stick-slip friction to evaluate the corrugation amplitude of the surface potential [14,16,19]. Here, to obtain c_{eff} and a, further model analyses are needed, as their quantitative evaluation is not that straightforward [21]. As a matter of fact, this would give access to the initial barrier height induced by puckering on each domain.

To gain insight into this mechanism, we calculate the mean lateral tip position needed to induce a slip on each domain and compare it with the variation of the slip height plotted in Fig. 3(d). To do so, we first estimate a mean value of D for various domains—from images acquired with the same tip and under similar scan conditions—as follows: $\langle D \rangle = P/\sin\theta$, where P is again the periodicity of the stripes obtained by FFT analyses. Then, a good approximation is that $\langle D \rangle$ also corresponds to the distance traveled by the tip along the stiff direction. This is supported by the constant slopes measured during the stick phases [Figs. 3(a) and 3(b)]. The mean lateral tip position with respect to the scan direction is then $\langle D \rangle(\theta) \times \sin[(\pi/2) - \theta]$. Its variation as a function of θ is shown in Fig. 4(b). The good qualitative agreement with the plot in Fig. 3(d) suggests that the local orientation of the stiff direction is indeed the main cause for the various frictional domains observed here [Fig. 1(a)].

Additionally, the inset of Fig. 4(b) shows that $P(\theta)$ presents two marked discontinuities at 30° and 60°. This, again, can be understood by assigning an enhanced stiffness to one particular high-symmetry axis. The two sets of directions of the honeycomb lattice (3 × zigzag and 3 × armchair) rotated each other by 30° are known to have different elastic characteristics [22,23]. Thus, depending on the angular sector spanned by the stiff direction [orange intervals in Fig. 4(c)], $P(\theta)$ is expected to show a periodicity of 60°. Nevertheless, these minute effects are too weak to induce abrupt discontinuities in the variation of slip height [Fig. 3(d)] or of mean lateral tip position Fig. 4(b)] where they are smeared out by the sinus function.

The above scenario naturally gives rise to a question: why is one particular direction privileged over the other two of equivalent symmetry and ultimately responsible for this friction mechanism? We find that the puckering friction is, in fact, a sensitive probe for local deformation fields at the graphite surface (see Sec. 2 in Ref. [12]). These fields, which usually arise from structural defects such as dislocations, grain boundaries, or pinnings at step edges, locally may break the crystal symmetry stiffening one particular direction [24]. This is supported by the observation of 60° reorientation of the stripes on atomic terraces belonging to the same crystal grains (see Ref. [12], Fig. 2). Note that this defect-induced friction change described here is at variance with the friction mechanism proposed for rippled graphene [11], where anisotropic puckering is

driven by intrinsic ripples (out-of-plane topographic modulations), which obviously do not exist at the graphite surface.

In conclusion, we evidence a friction mechanism relevant for nanoscale frictional characteristics of graphite. The mechanism relies on the competition between the stiffness difference of crystal lattice and local deformation fields induced by structural defects. The results reported here may open the exciting perspective of tuning friction in sliding nanoscale contacts. Our findings also provide a fresh insight into frictional properties of graphite, and we believe this gives a new thrust in the study of friction on lamellar materials.

*rastei@ipcms.unistra.fr

[1] J. Y. Park, D. F. Ogletree, P. A. Thiel, and M. Salmeron, Science **313**, 186 (2006).
[2] R. Cannara, M. J. Brukman, K. Cimatu, A. V. Sumant, S. Baldelli, and R. W. Carpick, Science **318**, 780 (2007).
[3] T. Filleter, J. L. McChesney, A. Bostwick, E. Rotenberg, K. V. Emtsev, T. Seyller, K. Horn, and R. Bennewitz, Phys. Rev. Lett. **102**, 086102 (2009).
[4] S. Morita, S. Fujisawa, and Y. Sugawara, Surf. Sci. Rep. **23**, 1 (1996).
[5] C. M. Mate, G. M. McClelland, R. Erlandsson, and S. Chiang, Phys. Rev. Lett. **59**, 1942 (1987).
[6] M. Dienwiebel, G. S. Verhoeven, N. Pradeep, J. W. M. Frenken, J. A. Heimberg, and H. W. Zandbergen, Phys. Rev. Lett. **92**, 126101 (2004).
[7] Z. Liu, J. Yang, F. Grey, J. Z. Liu, Y. Liu, Y. Wang, Y. Yang, Y. Cheng, and Q. Zheng, Phys. Rev. Lett. **108**, 205503 (2012).
[8] A. Socoliuc, R. Bennewitz, E. Gnecco, and E. Meyer, Phys. Rev. Lett. **92**, 134301 (2004).
[9] S. Cahangirov, C. Ataca, M. Topsakal, H. Sahin, and S. Ciraci, Phys. Rev. Lett. **108**, 126103 (2012).
[10] C. Lee, Q. Li, W. Kalb, X.-Z. Liu, H. Berger, R. W. Carpick, and J. Hone, Science **328**, 76 (2010).
[11] J. S. Choi, J.-S. Kim, I.-S. Byun, D. H. Lee, M. J. Lee, B. H. Park, C. Lee, D. Yoon, H. Cheong, K. H. Lee, Y.-W. Son, J. Y. Park, and M. Salmeron, Science **333**, 607 (2011).
[12] Supporting data are available in the Supplemental Material at http://link.aps.org/supplemental/10.1103/PhysRevLett.111.084301.
[13] Y. Sang, M. Dubé, and M. Grant, Phys. Rev. Lett. **87**, 174301 (2001).
[14] A. Schirmeisen, L. Jansen, and H. Fuchs, Phys. Rev. B **71**, 245403 (2005).
[15] Y. Sang, M. Dubé, and M. Grant, Phys. Rev. E **77**, 036123 (2008).
[16] L. Jansen, H. Hölscher, H. Fuchs, and A. Schirmeisen, Phys. Rev. Lett. **104**, 256101 (2010).

[17] P. Hänggi, P. Talkner, and M. Borkovec, Rev. Mod. Phys. **62**, 251 (1990).

[18] A. Garg, Phys. Rev. B **51**, 15 592 (1995).

[19] E. Riedo, E. Gnecco, R. Bennewitz, E. Meyer, and H. Brune, Phys. Rev. Lett. **91**, 084502 (2003).

[20] E. Gnecco, R. Bennewitz, T. Gyalog, Ch. Loppacher, M. Bammerlin, E. Meyer, and H.-J. Güntherodt, Phys. Rev. Lett. **84**, 1172 (2000).

[21] A direct use of Hooke's law to extract c_{eff} from stick phases is misleading here, as the friction force is noncollinear with the displacement. Additionally, a is no longer the interatomic distance used in the Prandtl-Tomlinson model of atomic friction. Here, it is rather related to the width of the puckered region, which obviously needs further modeling to be evaluated.

[22] V. M. Pereira, A. H. Castro Neto, and N. M. R. Peres, Phys. Rev. B **80**, 045401 (2009).

[23] A. Sakhaee-Pour, Solid State Commun. **149**, 91 (2009).

[24] Strain fields induced by structural defects are currently of high research interest, see, for instance, J. H. Warner, E. R. Margine, M. Mukai, A. W. Robertson, F. Giustino, and A. I. Kirkland, Science **337**, 209 (2012).